ELSEVIER

Robotics and Autonomous Systems 13 (1994) 87–95

Robotics and Autonomous Systems

Depth estimation from a sequence of monocular images with known camera motion

Hanqi Zhuang *, R. Sudhakar, Jen-yu Shieh

Dept. of Electrical Engineering, Florida Atlantic University, P.O. Box 3091, Boca Raton, FL 33431-0991, USA

Communicated by T.C. Henderson
Received August 15, 1992; revised September 5, 1993

Abstract

This paper reports an approach of computing depth maps from a monocular image sequence, under the assumption that the camera motion is known. The direct depth estimation method is combined with the optical flow based method to improve estimation accuracy. The optical flow on and near moving edges are computed using a correlation technique. The optical flow information is then fused with gradient information to estimate depth not only on the moving edges but also in the internal regions. The depth estimation problem is formulated as a Kalman filter problem and is solved in three stages. In the prediction stage, the depth map estimated for the current frame, together with knowledge of the camera motion, is used to predict the depth and depth variance at each pixel in the next frame. In the estimation stage, a Kalman filter is employed to refine the predicted depth map. The resulting estimation algorithm takes into account the information from the neighboring pixels. In the smoothing stage, based on the error covariance information, morphological filtering is applied to reduce the effect of measurement noise and to fill in untrustable areas. Simulation results are provided to demonstrate the effectiveness of the proposed method.

Key words: Depth estimation; Kalman filtering; Optical flow; Autonomous navigation

1. Introduction

In many applications involving autonomous navigation, robot vision and surveillance, there is a need for determining the depth map. Depth can be estimated by using stereo cameras [1–3], by changing focal length [4,5], by using a plenoptic camera [6], or by employing moving cameras [7–17]. In this paper we are concerned with the problem of recovering depth maps from a sequence of monocular images of the object assuming that the relative motion between the object and the camera is known.

Depth may be estimated based on two frames or multiple frames. A single snapshot of two frames may not provide sufficient information for accurate depth estimation. Use of multiple frames improves the accuracy, reduces the influence of noise and allows the extraction of additional information which cannot be recovered from just two frames [10–14]. The available depth/structure estimation methods based on Kalman filtering use feature matching [11], moving cam-

* Corresponding author.

0921-8890/94/$07.00 © 1994 Elsevier Science B.V. All rights reserved
SSDI 0921-8890(93)E0035-L

IPR2026-0300
Zinser Exhibit 2034, Page 1 of 9

era images [13], optical flow [10,12], and direct method of Horn [14].

In the proposed scheme, we combine the direct depth estimation method with the optical flow based method to improve the overall estimation accuracy. Typically, the gradient information is very sensitive to noise along moving edges. On the other hand, the optical flow based method is computationally more expensive and is not reliable in internal regions. We compute optical flow only around edges and then combine with gradient information to recover depth not only on the moving edges but also in the internal regions.

The depth estimation problem is formulated as a discrete Kalman filter problem [18] and is solved in three stages. In the prediction stage, the depth map estimated for the current frame, together with knowledge of the camera motion, is used to predict the depth and depth variance at each pixel in the next frame. In the estimation stage, a vector-version of Kalman filter formulation is adopted and then simplified to refine the predicted depth map. The optical flow information on and near moving edges and gradient information in the internal regions are combined in this stage. Since the resulting estimation algorithm takes into account the information from the neighboring pixels, it is much more robust than the scalar-version Kalman filter implementation. In the smoothing stage, based on the error covariance information, morphological filtering [19] is applied to the estimated depth map to reduce the measurement noise and to fill in untrustable areas. We choose morphological filtering which preserves edges while smoothing the depth map.

2. Problem formulation

As an image sequence provides only partial information about the scene, it is necessary to have assumptions about the scene and its 2-D images. We assume that (1) camera motion is known, (2) the object is a rigid body, (3) the image is changing slowly in two successive frames, and (4) in a small internal of time, the brightness of a given object point is unchanged. The algorithms based on gradient and optical flow are formulated as follows.

2.1. Gradient based method

The brightness change Eq. (1) is the basis for the proposed depth estimation method [20]. We rewrite the brightness change equation as a dynamic model and apply the Kalman filter algorithm to do recursive depth estimation from the image sequence. For the simplification of the notation, the dependence of the variables Z, s, ν, E_x, E_y, and E_t on image coordinates x and y are suppressed. The depth Z corresponding to an image point (x, y) is given by [20]

$$Z = -\frac{s \cdot T}{E_t + \nu \cdot \Omega} \tag{1}$$

where E_t is the brightness temporal derivative, $T = [U, V, W]^T$ is the translation vector, $\Omega = [A, B, C]^T$ is the rotation vector,

$$s \triangleq \begin{bmatrix} -fE_x \\ -fE_y \\ xE_x + yE_y \end{bmatrix}, \tag{2}$$

and

$$\nu \triangleq \begin{bmatrix} fE_y + \frac{y}{f}(xE_x + yE_y) \\ -fE_x - \frac{x}{f}(xE_x + yE_y) \\ yE_x - xE_y \end{bmatrix}. \tag{3}$$

Here E_x and E_y are the brightness spatial derivatives, and f is the focal lens of the camera. Note that s and ν weigh the contribution of T (translation) and Ω (rotation) vector. We define the parameters:

$$\begin{aligned} \xi_k &\triangleq Z_k, \\ \eta_k &\triangleq (s \cdot T)_k, \\ h_k &\triangleq -(\nu \cdot \Omega + E_t)_k, \end{aligned} \tag{4}$$

where the subscript 'k' denotes the quantities in the kth estimation stage. These will be used to construct a system equation in Section 2.3.

IPR2026-0300
Zinser Exhibit 2034, Page 2 of 9

2.2. Optical flow based method

The optical flow equation is given by [21]

$$u = \frac{-fU + xW}{Z} + \frac{1}{f}\left(Axy - B(x^2 + f^2) + Cyf\right),$$
$$v = \frac{-fV + yW}{Z} + \frac{1}{f}\left(A(y^2 + f^2) - Bxy - Cxf\right), \tag{5}$$

where u and v are the image velocities along the x and y directions, respectively. These motion field equations can be established at every pixel (x, y) in the image plane. We define the parameters as

$$\xi_k \triangleq Z_k,$$
$$\eta_k \triangleq \frac{1}{2}\left[\frac{-fU + xW}{u - \frac{1}{f}\left(Axy - B(x^2 + f^2) + Cyf\right)} + \frac{-fV + yW}{v - \frac{1}{f}\left(A(y^2 + f^2) - Bxy - Cxf\right)}\right]_k,$$
$$h_k \triangleq 1. \tag{6}$$

Again these will be substituted into (7) and (8) to form a system model.

2.3. System model

A state space representation of either Eq. (4) or (6) can be given as

$$\xi_{k+1} = a_k \xi_k + w_k, \quad w_k \sim N(0, q_k), \tag{7}$$
$$\eta_k = h_k \xi_k + v_k, \quad v_k \sim N(0, r_k), \tag{8}$$

where a_k is the time-variant state transition coefficient which reflects the variation of depth with motion, which can be determined from the known motion parameters in the prediction stage, and w_k and v_k are zero mean white noises, uncorrelated with each other and with ξ_0.

The depth, expressed as a state variable(ξ_k), may be estimated using information from the neighboring pixels to reduce noise effects. Hence, Eq. (8) is rewritten in its vector form.

$$Y_k = H_k \xi_k + V_k, \quad V_k \sim N(0, R_k), \tag{9}$$

where

$$H_k = [h_k(1)\ h_k(2)\ \ldots\ h_k(m)]^t; \tag{10}$$
$$V_k = [v_k(1)\ v_k(2)\ \ldots\ v_k(m)]^t; \tag{11}$$

and each h_k has a structure given in (4) or (6), depending on whether the estimation is made on the edges or not; m is the number of pixels used to compute ξ_k, and R_k is the $m \times m$ covariance matrix. The state space model given in eqs. (7) and (8) will be used to update the depth map.

3. Prediction stage

The task of the prediction stage is to predict the depth and its variance after motion, i.e., how it appears to the observer at time $k + 1$ based on the depth and variance at time k. We present an algorithm which is different from those outlined in [12,14].

3.1. Depth prediction

We would like to predict the object point corresponding to the image point $(x_{i,j}, y_{i,j})$ at frame $k + 1$ using the depth information at frame k and known camera motion parameters. The object points corresponding to the image point $(x_{i,j}, y_{i,j})$ as well as its two neighboring points $(x_{i,j+1}, y_{i,j-1})$ and $(x_{i+1,j}, y_{i+1,j})$ at frame k are obtained through the perspective projection.

Let us denote the corresponding object points at frame k by $(X_{i,j}, Y_{i,j}, Z_{i,j})$, $(X_{i,j+1}, Y_{i,j+1}, Z_{i,j+1})$, and $(X_{i+1,j}, Y_{i+1,j}, Z_{i+1,j})$ (or in short $(R_1, R_2, R_3)_k$). The locations of these object points at frame $k + 1$ are predicted using the known camera motion parameters. Let the new locations of these object points at frame $k + 1$ be $(X'_{i,j}, Y'_{i,j}, Z'_{i,j})$, $(X'_{i,j-1}, Y'_{i,j+1}, Z'_{i,j+1})$, and $(X'_{i+1,j}, Y'_{i+1,j}, Z'_{i+1,j})$ or in short $(R_1, R_2, R_3)_{k+1}$. A plane, say Plane A, is constructed to pass through $(R_1, R_2, R_3)_{k+1}$. Assume that the object point $(X'_{i,j}, Y'_{i,j}, Z'_{i,j})$ of the image point $(x_{i,j}, y_{i,j})$ at frame $k + 1$ lies on Plane A. Then the 3-D coordinates of the object point $(X'_{i,j}, Y'_{i,j}, Z'_{i,j})$ is the intersection of the focal ray with Plane A. $Z'_{i,j}$ is the predicted depth. Figs. 1 and 2 respectively

IPR2026-0300
Zinser Exhibit 2034, Page 3 of 9

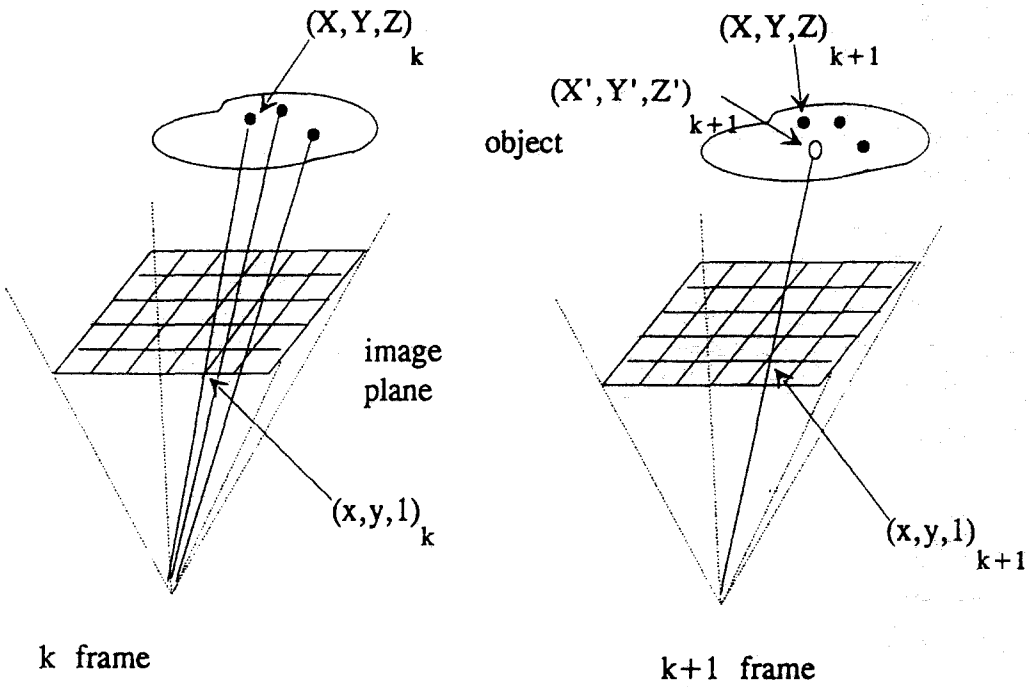


Fig. 1. Depth prediction schematics.

provide the illustration and block diagram of the depth prediction scheme. The prediction algorithm is given below.

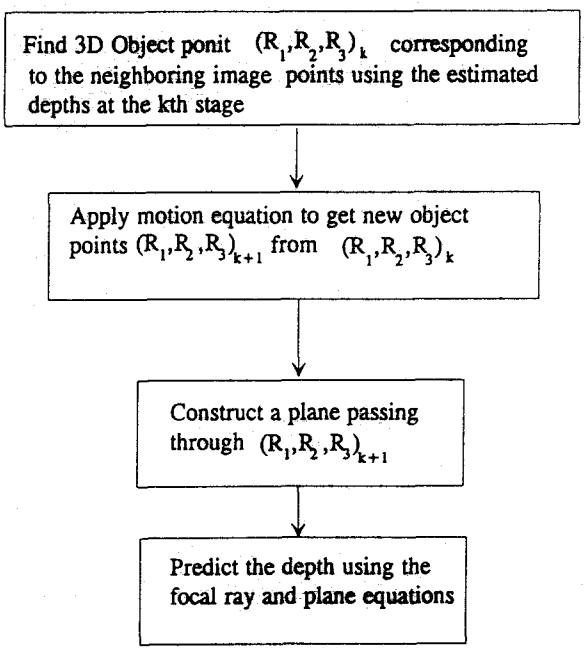


Fig. 2. Procedure for depth prediction at each pixel.

3.2. Prediction algorithm

1. Using perspective projection equations, we compute the object point for each pixel of image frame k. For the ijth pixel, we consider the set of three points in the triangular neighborhood, namely $\{(i, j), (i, j+1)$ and $(i+1, j+1)\}$. The object point coordinates are obtained using the focal ray equations,

$$X_{ij} = \frac{x_{ij} Z_{ij}}{f}, \quad Y_{ij} = \frac{y_{ij} Z_{ij}}{f}, \tag{12}$$

where Z_{ij} is the estimated depth in the kth stage at the image coordinates (i, j). We denote the three object points by $(R_1, R_2, R_3)_k$.

2. Using the known motion parameters, we determine the new position of the three object points at the instant of frame $k+1$. That is,

$$\begin{bmatrix} X'_{i,j} \\ Y'_{i,j} \\ Z'_{i,j} \end{bmatrix} = - \begin{bmatrix} U \\ V \\ W \end{bmatrix} - \begin{bmatrix} 1 & -C & B \\ C & 1 & -A \\ -B & A & 1 \end{bmatrix} \begin{bmatrix} X_{i,j} \\ Y_{i,j} \\ Z_{i,j} \end{bmatrix}. \tag{13}$$

IPR2026-0300
Zinser Exhibit 2034, Page 4 of 9

Again we denote the three points by $(R_1, R_2, R_3)_{k+1}$.

3. Plane A which passes through the three points $(R_1, R_2, R_3)_{k+1}$ is then constructed. Let the plane be defined by

$$Z = aX + bY + c. \tag{14}$$

4. Find the intersection of focal ray through grid point (x, y) and the constructed plane. Using (12) and (14), one obtains

$$Z'_{ij} = \frac{c}{1 - \frac{a}{f}x_{ij} - \frac{b}{f}y_{ij}}, \tag{15}$$

where Z'_{ij} is the predicted depth value in frame $k+1$ for the image point $(x_{i,j}, y_{i,j})$.

There is a singular case in the construction of the plane. If the three projected object points are in a straight line, say Line A, there is no unique plane. In other words, the focal ray does not necessary intersect Line A. A possible solution is to find the common normal between the focal ray and line A. The common normal is unique since Line A cannot be parallel to the focal ray. The intersection of the focal ray with the common normal can be used as the predicted object point at frame $k+1$ for the (i, j)th image point.

Using the Kalman filter algorithm [18], we have the time updates for depth (ξ_{k+1}) and its covariance (p^-_{k+1}) as

$$\begin{aligned} \xi^-_{k+1} &= a_k \xi_k, \\ p^-_{k+1} &= a_k^2 p_k + q_k, \end{aligned} \tag{16}$$

where the grid indices (i, j) have been omitted, a_k is computed by

$$a_k = \frac{Z'_{ij}}{Z_{ij}}. \tag{17}$$

Again, the dependence of the variables ξ_k, p_k, and a_k in (16) and (17) on image coordinates are suppressed. After a_k is computed, the time update covariance p^-_{k+1} is obtained from p_k. The process noise (w_k) is measured from the change of depth over time. The process noise depends on the derivation of the object surface from the fitted plane. If all the object points lie on the plane, the prediction error is zero. Therefore the process noise is proportional to the fitting residual which can be obtained with more than three object points.

4. Estimation stage

If the rigid body motion vectors T and Ω are known, the brightness change constraint equation or optical flow equation contains only one unknown variable, the depth, which can be solved easily. After the kth image frame is available, we compute the temporal and spatial gradients or the optical flow around edges, which can be then used to update Z_k based on the Kalman filter update rule. In the simplest case, the depth Z could be updated using a scalar-version of Kalman filter. However, since the gradient information is very sensitive to noise, a vector-version Kalman filter performs better. In this stage, the edge information is used to choose filter equations. If an edge is detected, the optical flow Eq. (6) is employed. Otherwise the gradient Eq. (4) is selected.

4.1. Kalman filter

The measurement update equation of the Kalman filter algorithm [18] is:

$$\begin{aligned} \xi_{k+1} &= \xi^-_{k+1} + K_{k+1}[\eta_{k+1} - H_{k+1}\xi_{k+1}], \\ P_{k+1} &= [I - K_{k+1}H_{k+1}]P^-_{k+1}, \end{aligned} \tag{18}$$

where,

$$K_{k+1} = P_{k+1}H^{\mathrm{T}}_{k+1}R^{-1}_{k+1}. \tag{19}$$

We assume that the depth at the image coordinates (i, j) is estimated using measurements from an $L \times L$ neighborhood W centered at (i, j). Denote the covariance of the depth estimates at the m pixels in W (row-scanned), by $r(l)$, $l = 1, \ldots, m$, where $m = L \times L$ and L is the size of the window. For example, if we choose $L = 3$, $r(5)$ is the variance of Z_{ij} due to the uncertainty of the measurement at (i, j) and $r(1) \ldots r(4)$, $r(6) \ldots r(9)$ are the covariances representing the uncertainties caused by neighborhood measurements.

IPR2026-0300
Zinser Exhibit 2034, Page 5 of 9

As the scalar estimate of ξ_k is made using the measurement from all pixels of the $(L \times L)$ neighborhood, their errors can be assumed to be uncorrelated. Thus for each pixel (i, j) in frame k, R_k can be defined as:

$$R_k = \mathrm{diag}[r_k(1)\ r_k(2)\ \ldots\ r_k(m)]^{\mathrm{T}}, \tag{20}$$

where $m = L \times L$. Using (20), (19) and (10) to simplify (18), one has,

$$P_{k+1} = \frac{P_{k+1}^-}{1 + P_{k+1}^- \sum_{i=1}^{m} h_{k+1}(i)^2 / r_{k+1}(i)}. \tag{21}$$

Thus the measurement update of the depth estimate is:

$$\xi_{k+1} = \xi_{k+1}^- + P_{k+1}\left[\sum_{i=1}^{m} h_{k+1}(i)\frac{1}{r_{k+1}(i)}(\eta_{k+1}(i) - h_{k+1}(i)\xi_{k+1}^-)\right]. \tag{22}$$

Complex matrix inversions are avoided due to the particular structure of R_k.

The measurement covariance matrix R_k represents the measurement noise which includes, (1) the uncertainties in the computation of temporal and spatial gradients, (2) the uncertainties due to the linear approximation in the derivation of the brightness change equation, and (3) the mismatching in the correlation process for optical flow computation. For a detailed account of the covariance matrix derivation and optical flow computation procedure, readers are referred to [22,23].

5. Smoothing stage

This stage is devoted for the improvement of the depth estimation in the region where image points have high variances. Depth estimates of zero and negative values are certainly incorrect. In high variance regions for which the estimates do not change from their initial values, we need to do surface interpolation to improve the depth estimation [12,19,24].

To this end, we use a fill-in algorithm along with morphological filters to smooth the depth map. We choose the close-open filter [24], which has the property of noise suppression. Before performing the close–open operation, depths in high variance regions are replaced by their neighboring depth values using a fill-in algorithm. The fill-in algorithm is a recursive cross-shaped filter which retains edges and is inexpensive to compute. The algorithm is outlined below [22]:

1. Start with window size $N = 3$. If the number of trustable depth values of a window of size $2N - 1$ is greater than N, replace the pixel value by the median value.
2. Else increase the window size to $N + 2$. If $N < N_{\max}$, where $N_{\max}$ is a prescribed number, go to step 1. Else go step 3.
3. Extend the window size further up to $N_{\max}$. Then replace the depth value by the median value in the window.

6. Simulation results

Both synthetic and real images were tested for the proposed Kalman filter multiframe algorithm. For the first experiment, 256×256 images of a moving planar object superimposed with a sinusoidal pattern were generated using a camera model given in [25]. The motion vectors were $T = [0.5\ 0\ 0]$ mm and $\Omega = [0\ 0\ 0]$ rad. between two consecutive frames. Noise was added to image brightness to test the robustness of the algorithm. Figs. 3 and 4 show the estimated depth map of the planar object from a sequence of 9

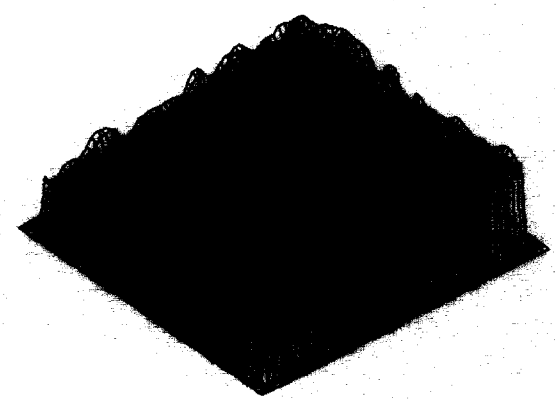


Fig. 3. Estimation result of a planar surface with SNR = 10.

IPR2026-0300
Zinser Exhibit 2034, Page 6 of 9

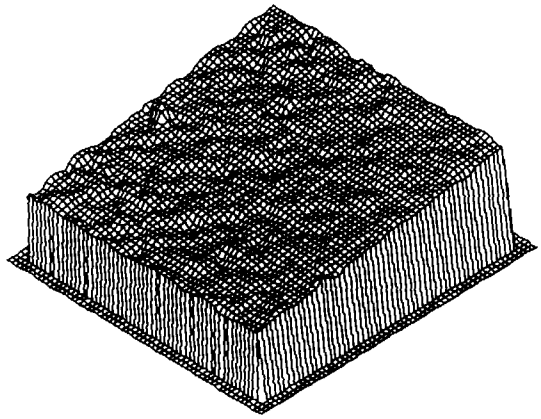


Fig. 4. Estimation result of a planar surface with SNR = 80.

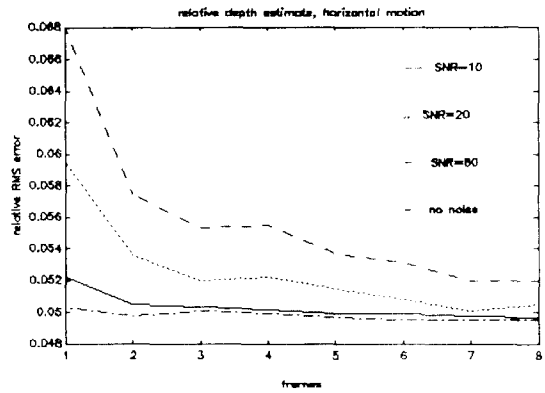


Fig. 6. Algorithm convergence rate (horizontal motion).

images added with different level of Gaussian noise (signal to noise ratio, SNR = 10, 80). Figs. 5 and 6 illustrate the convergence nature of the parameter estimation under different noise levels. As expected, the estimates become more accurate with increased SNR. Fig. 7 shows the nonplanar surface generated for the second experiment. Fig. 8 presents the depth map estimated using 9 frames of horizontal motion without noise.

In the experiment with real images, a sequence of eleven 128×128 images of a moving golf ball were obtained using a CCD camera attached to an Image Technology Frame Grabber installed in an IBM PC AT. The golf ball was set about 940 mm from the camera. The motion vectors were $T = [0.5\ 0.5\ 0]$ mm and $\Omega = [0\ 0\ 0]$ rad. between two consecutive frames. The Kalman filter was

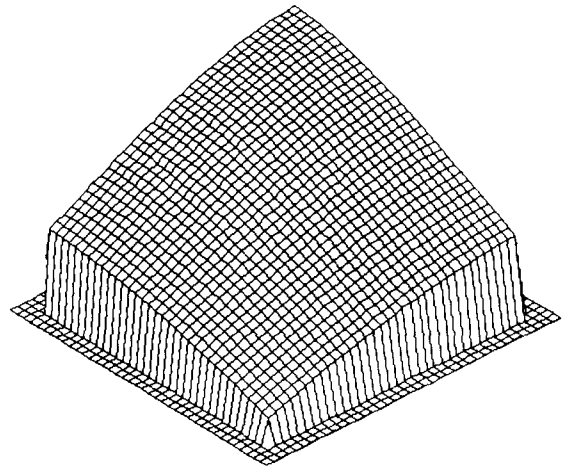


Fig. 7. A 3D surface generated by computer.

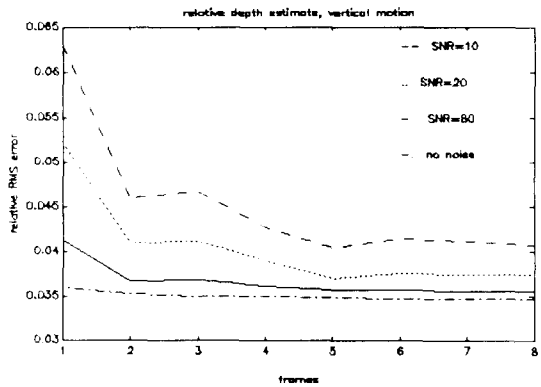


Fig. 5. Algorithm convergence rate (vertical motion).

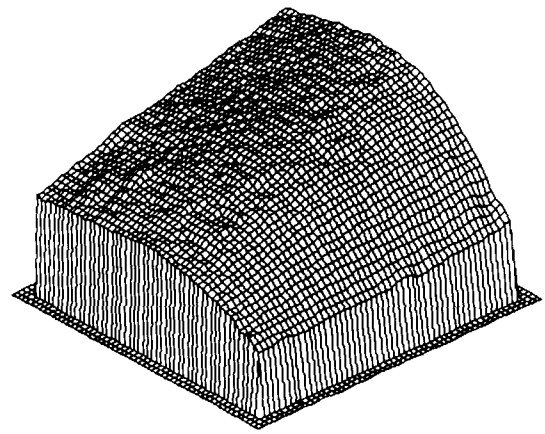


Fig. 8. The estimated depth map using 9 frames.

IPR2026-0300
Zinser Exhibit 2034, Page 7 of 9

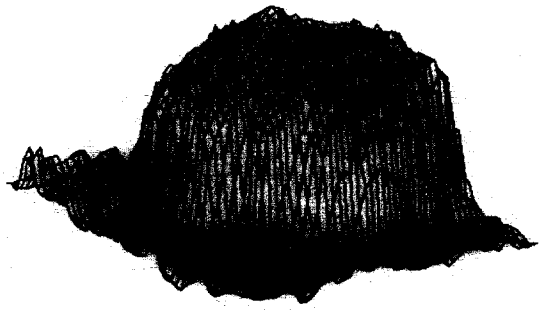


Fig. 9. Estimated 3D depth map using optical flow and gradient information.

initialized with $Z_0 = 940$ and $p_0 = 300{,}000$. In the measurement stage, a 3×3 window was used to compute neighborhood points. In the smoothing stage, the close-opening filter with a 9×9 window was used to do surface interpolation. No reliable depth information can be obtained from motion in the region of uniform brightness. Fig. 9 shows the estimated 3D depth using both the optical flow and gradient information, while Fig. 10 illustrates the result obtained without using the optical flow information.

7. Conclusion

A Kalman filter algorithm with new prediction and smoothing procedures is presented for the estimation of depth from image sequences. The algorithm can recover depth information along object boundaries. The highlights of the algorithm are as follows: In the prediction stage a resampling and extrapolation method is used to avoid image warping that is computationally very expensive. In the estimation stage both the optical flow around edge and the gradient information from the whole region are selectively combined. Depth estimation is improved by using information from the neighboring regions. This step takes into account measurement uncertainties from neighboring pixels. It is performed through a vector-version Kalman filter which does not require any matrix inversions and is computationally simple. In the smoothing stage, morphological filtering is performed on the estimates to recover the depth along object boundaries. Since the depth at each pixel is estimated locally, the algorithm presented in this paper can be speeded up by implementing on a parallel computer.



Fig. 10. Estimated 3D depth map only using gradient information.

References

[1] W.E.L. Grimson, *From Images to Surfaces: A Computational Study of the Human Early Visual System*, (MIT, Cambridge, MA, 1981).

[2] M. Ito and A. Ishii, Three view stereo analysis, *IEEE Trans. Patt. Anal. Machine Intell.* PAMI-8 (1986) 524–531.

[3] N. Ayache and F. Lustman, Fast and reliable passive trinocular stereo-vision, *Proc. ICCV*, 422–427.

[4] A.P. Pentland, A. new sense for depth of field, *IEEE Trans. Patt. Anal. Machine Intell.* PAMI-9 (1987) 523–531.

[5] V.M. Bove, Jr., Probabilistic method for integrating multiple sources of range data, *J. Opt. Soc. Amer.* A-7 (1990) 2193–2207.

[6] E.H. Adelson and J.Y.A. Wang, Single lens stereo with a plenoptic camera, *IEEE Trans. Patt. Anal. Machine Intell.* PAMI-14 (2) (1992) 99–106.

[7] R.C. Bolles, H.H. Baker and D.H. Marimont, Epipolar-plane image analysis: An approach to determining structure from motion, *Int. J. Comp. Vis.* 1 (1987) 7–55.

[8] G. Adiv, Determining three-dimensional motion and structure from optical flow generated by several moving objects, *IEEE Trans. Patt. Anal. Machine Intell.* PAMI-7 (4) (1985) 384–401.

[9] J. Weng, T.S. Huang and N. Ahuja, 3-D motion estimation, understanding, and prediction from noisy image sequences, *IEEE Trans. Patt. Anal. Machine Intell.* PAMI-9 (3) (1987) 370–389.

[10] T.J. Broida and R. Chellappa, Estimation of object motion parameters from noise images, *IEEE Trans. Patt. Anal. Machine Intell.* PAMI-8 (1) (1986) 90–99.

[11] S. Bharwani, E. Riseman and A. Hanson, Refinement of

IPR2026-0300
Zinser Exhibit 2034, Page 8 of 9

environment depth maps over multiple frames, *Proc. Workshop on Motion: Representation and Analysis*, Charleston, SC (May 1986) 73–80.

[12] L. Matthies, T. Kanade and R. Szeliski, Kalman filter-based algorithms for estimating depth from image sequences, *Int. J. Comp. Vis.* 3 (1989) 209–236.

[13] H.H. Baker and R.C. Bolles, Generalizing Epipolar-plane image analysis on the spatiotemporal surface. *Int. J. Comp. Vis.* 3 (1989) 33–49.

[14] J. Heel, Direct estimation of structure and motion from multiple frames, AI Memo 1190, MIT Artificial Intelligence Laboratory, March 1990.

[15] Y.C. Kim, Finding range from stereo images, *IEEE Computer Society Conf. Computer Vision and Pattern Recognition*, San Francisco, CA (1985) 289–294.

[16] R. Nevatia, Depth measurement by motion stereo, *Computer Graphics and Image Processing* 5 (1976) 203–214.

[17] W. Richards, Structure from stereo and motion. *J. Opt. Soc. Amer.* 2 (1985) 343–349.

[18] Frank L. Lewis, *Optimal Estimation with an Introduction to Stochastic Control Theory* (Wiley, New York, 1986).

[19] D. Geiger and F. Girosi, Parallel and deterministic algorithms for MRFS: Surface reconstruction and integration. AI Memo 1114, MIT Artificial Intelligence Laboratory, June 1989.

[20] B.K.P. Horn and E.J. Weldon Jr., Direct methods for recovering motion, *Int. J. Comp. Vis.* 2 (1988) 51–76.

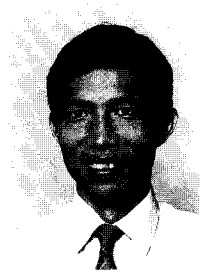
[21] B.K.P. Horn, *Robot Vision* (MIT Press, Cambridge, MA, 1986).

[22] J. Shieh, Structure and motion estimation from image sequences, Ph.D. Dissertation, Florida Atlantic University, 1992.

[23] J. Shieh, H. Zhuang and R. Sudhakar, Motion estimation from a sequence of stereo images: A direct method, to appear in *IEEE Trans. Systems, Man, and Cybernetics*.

[24] P. Maragos and R.W. Schafer, Morphological filters – Part I: Their set-theoretic analysis and relations to linear shift-invariant filters, *IEEE Trans. on Acoustics, Speech, and Signal Processing* ASSP-35 (8) (1987) 1153–1168.

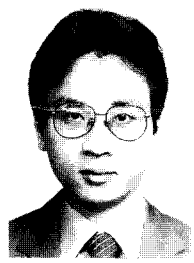
[25] R.Y. Tsai, A versatile camera calibration technique for high-accuracy 3D machine vision metrology using off-the-self TV cameras and lenses, *IEEE J. Robotics and Automation* RA-3 (4) (1987).



Hanqi Zhuang received the B.S. degree in Engineering from Shanghai University of Technology in 1982, and the M.S. and Ph.D. degrees in Electrical Engineering from Florida Atlantic University in 1986 and 1989, respectively. While completing his M.S. and Ph.D. degrees at FAU, he was a Research Assistant for the Robotics Center, working on Robot Calibration and Computer Vision. Since December 1989, he has been a faculty member in the Department of Electrical Engineering, where he is now an Assistant Professor. His current research interests include robotics, computer vision, computer-integrated manufacturing, and lasers and optics. Dr. Zhuang is a senior member of IEEE.



R. Sudhakar received his B.Sc. (Engg.) degree in Electronics and Communications Engineering from the University of Kerala, India, in 1973, the M. Tech degree in Radar and Communication Engineering from the Indian Institute of Technology, Madras, India in 1977, and the Ph.D. degree for his research on Digital Signal Processing from the Indian Institute of Technology, New Delhi, India, in 1982. He joined Keltron, Trivandrum, India, in 1973. From 1982 to 1983 he was with the University of Rhode Island, Kingston, as a post-doctoral fellow. Since August 1983, he has been with the Florida Atlantic University, Boca Raton, currently as an Associate Professor in Electrical Engineering. His research interests are in signal processing, digital communications, and computer vision. Dr. Sudhakar is a Professional Engineer in the state of Florida.



Jen-yu Shieh received the M.S. degree in Engineering from the Department of Computer Science and Engineering and the Ph.D. degree in Electrical Engineering from the Department of Electrical Engineering, both at Florida Atlantic University in 1988 and 1992, respectively. While completing his Ph.D. degree at FAU, he was a Research Assistant for the Robotics Center, working on Vision-Based Depth and Motion Estimation. Since January 1993, He has been an Associate Professor in National Yunlin Polytechnic Institute, Taiwan. His current research interests include computer vision and multimedia applications.

IPR2026-0300
Zinser Exhibit 2034, Page 9 of 9